frontiers in Chemical Engineering

TYPE Original Research
PUBLISHED 10 June 2026
DOI 10.3389/fceng.2026.1799905

OPEN ACCESS

EDITED BY
Jie Dong,
University of Georgia, United States

REVIEWED BY
Hu Li,
Guizhou University, China
Dewi Kurnianingsih Arum Kusumahastuti,
Satya Wacana Christian University,
Indonesia

*CORRESPONDENCE
Philipp M. Grande,
p.grande@fz-juelich.de
Holger Klose,
h.klose@fz-juelich.de

†These authors have contributed equally to this work and share first authorship

RECEIVED 30 January 2026
REVISED 24 April 2026
ACCEPTED 06 May 2026
PUBLISHED 10 June 2026

CITATION
Uellendahl K, Reinwarth J, Haaf M, Grande PM and Klose H (2026) Biorefinery potential of paludiculture biomass: composition and fractionation analysis of *Phragmites*, *Phalaris*, and *Carex*. *Front. Chem. Eng.* 8:1799905. doi: 10.3389/fceng.2026.1799905

Biorefinery potential of paludiculture biomass: composition and fractionation analysis of *Phragmites*, *Phalaris*, and *Carex*

Kora Uellendahl[1,2,3,4†], Judith Reinwarth[1,2†], Merlin Haaf[1,2], Philipp M. Grande[1,4*] and Holger Klose[1,2,4*]

[1]Institute of Bio- and Geosciences: Plant Sciences (IBG-2), Forschungszentrum Jülich GmbH, Jülich, Germany, [2]Rheinisch-Westfälische Technische Hochschule (RWTH) Aachen, Aachen, Germany, [3]University of Greifswald, Greifswald, Germany, [4]Bioeconomy Science Center (BioSC), Jülich, Germany

Peatlands store vast global carbon reserves but drainage for agriculture has turned them into major CO_2 sources. Full rewetting without alternative production systems would threaten farm incomes and regional value chains. Markets and value chains for biomass from rewetted peatlands are still largely undeveloped, and detailed knowledge of its chemical composition and suitability for integration into existing processing industries is lacking. In this study, we systematically investigated three dominant wetland taxa, *Phragmites australis*, *Phalaris arundinacea*, and *Carex* spp., alongside *Miscanthus* × *giganteus* as a benchmark, focusing on their lignocellulosic characterization, lignin structure, and the performance in OrganoCat fractionation. This study aims to provide a detailed compositional characterization of peatland grasses to establish their biomass potential for applications of bio-based value chains. The peatland grasses showed lower cellulose (25%–32% vs. 42%) and in case of *Carex* and *Phalaris* also lower lignin contents (18% vs. 24%) compared to *Miscanthus*. The hemicellulose profiles of *Miscanthus* and *Phragmites* were dominated by xylose and arabinose, whereas *Carex* and *Phalaris* exhibited more complex mixtures indicative of more highly substituted arabinoxylans or multiple polysaccharide classes. Lignin architecture also varied: lignin–carbohydrate complex (LCC) densities were up to 25% higher in peatland grasses compared to *Miscanthus*. *Phalaris* showed more condensed G-rich lignins (20% higher than in *Miscanthus*) and all peatland grasses showed a reduced S/G-ratio. *Carex* showed a higher ferulate content contrasting *Miscanthus'* less cross-linked structure. It was also demonstrated that the composition of lignin-bound polysaccharides varies substantially among the investigated grasses. Fractionation of the biomasses equilibrated the species-specific diversity of the four grasses, yielding cellulose-rich pulps with comparable composition (55%–65% cellulose) and saccharification efficiencies (>75%). This homogeneity across the processed pulps enables flexible mixed-species peatland biorefineries within multifunctional paludiculture systems prioritizing peat conservation and greenhouse gas mitigation.

KEYWORDS
bioeconomy, biorefinery, lignocellulose valorization, OrganoCat fractionation, lignin-carbohydrate complexes (LCC), peatland, paludiculture, saccharification

1 Introduction

Peatlands act as significant carbon stores, as while covering only about 3% of the global land surface, they contain about twice as much carbon as the biomass of all the world's forests combined (Parish, 2008; Yu, 2012). Yet, drainage for agriculture and forestry has turned these long-term sinks into major CO_2 sources, as in the absence of water, the carbon stored in the peat reacts with oxygen and is emitted as CO_2. Globally, emissions from drained peatlands account for an estimated 4% of all anthropogenic greenhouse gas emissions (Leifeld and Menichetti, 2018; UNEP, 2022). In certain regions like the peatland-rich federal states of Germany, drained peatlands can be responsible for nearly 40% of the state's emissions (Uellendahl et al., 2023). Rewetting drained peatlands can strongly reduce or even stop those emissions and, over time, re-establish carbon sequestration in litter and peat (Wilson et al., 2016), while simultaneously improving water retention, attenuating floods and droughts, providing local cooling, and restoring biodiversity and habitat functions (Bonn et al., 2014). As co-benefits of the resulting natural resources and products, these services can provide an important additional incentive for companies wishing to document their contributions to climate and nature conservation. However, a large share of drained peatlands in Europe and elsewhere is currently under intensive agricultural use (Böll-Stiftung, 2023; Wichmann and Nordt, 2024). Fully rewetting these areas without providing alternative production systems would undermine existing farm income and regional value chains, creating substantial social and economic barriers to implementation (Wichmann and Nordt, 2024).

Paludiculture, meaning productive agriculture and forestry on wet or rewetted peat soils, has been proposed as a key strategy to reconcile climate mitigation with continued land use (Wichtmann and Joosten, 2007). It maintains high water tables to conserve or even rebuild peat, while enabling biomass harvest from wetland-adapted species such as *Phragmites australis*, *Phalaris arundinacea*, *Carex* spp., and *Typha* spp. (Abel and Kallweit, 2022). Yet, for many of these "paludiculture crops" markets and value chains are still poorly developed. Missing value chains, missing economic incentives and agricultural policies are great obstacles for implementation (Ziegler et al., 2021). To integrate such climate-friendly feedstocks into existing industries, ranging from paper and fiber products to fine chemicals, a detailed understanding of their lignocellulosic cell-wall architecture is essential. These walls consist of cellulose microfibrils embedded within a matrix of non-cellulosic polysaccharides (mainly hemicellulose), with lignin providing structural reinforcement. In grasses, hemicellulose primarily comprises glucuronoarabinoxylans with varying substitution degrees, while lignin, composed of guaiacyl/syringyl units, forms cross-links via ferulates, p-coumarate esters and lignin–carbohydrate complexes (LCCs; Vogel, 2008; Giummarella et al., 2019). Biomass recalcitrance is tightly linked to cell-wall composition, polysaccharide-lignin cross-linking, and lignin structure, which together govern pretreatment severity, enzymatic deconstruction efficiency, and product yields in biochemical conversion routes (Himmel et al., 2007; Zeng et al., 2014; Klose and Paës, 2023). Moreover, lignin content, monomer composition (syringyl/guaiacyl/p-hydroxyphenyl ratio), and linkage types critically influence both pulping processability for fiber applications and the feasibility of lignin valorization routes in biorefineries (Ragauskas et al., 2014; Brienza et al., 2024; Schoofs et al., 2024). However, while several studies have explored the potential of paludiculture biomass for material or energy use, systematic investigations of its specific cell wall composition, lignin architecture and fractionation behavior remain scarce. Detailed characterization of paludiculture biomass thus underpins both techno-economic assessment and meaningful comparison with more established lignocellulosic feedstocks such as wood, straw, or energy grasses. In the broader context of lignocellulose biorefining, diverse fractionation strategies have been developed, for example, acid- and alkali-catalyzed pretreatments (Woiciechowski et al., 2020), deep eutectic solvents (DES; Liu et al., 2021), and organosolv processes such as OrganoCat (Grande et al., 2015), which vary in lignin removal selectivity and polysaccharide preservation.

This study specifically investigates how cell wall composition and lignin structure influence the fractionation behavior of dominant paludiculture species, *Phragmites australis*, *Phalaris arundinacea*, and *Carex* spp., in a mild organosolv system. By linking detailed chemical and structural analyses with quantitative assessments such as fractionation yield, composition of the fractions, and enzymatic saccharification efficiency, the work provides new insight into structure–process relationships of wetland biomass, a knowledge base not yet available for these species. As a reference benchmark for comparative analysis, *Miscanthus* × *giganteus* was selected because it represents an extensively studied, genetically stable, and partially commercialized energy crop with well-characterized lignocellulose structure, and composition, pulping behavior, and established biorefinery processability (Lewandowski et al., 2016; da Costa et al., 2017). With this, all grasses examined in this study belong to the order Poales, with *Carex* representing the Cyperaceae and all other grasses belonging to the Poaceae family. All biomasses were characterized with respect to their lignocellulosic composition and subsequently subjected to fractionation using the OrganoCat process, a biphasic acid-catalyzed organosolv system (Grande et al., 2015). This mild-condition fractionation strategy delivers three distinct product streams, cellulose-rich pulp (solid residue), hemicellulose-derived sugars (aqueous phase), and depolymerized lignin in the organic phase (Grande et al., 2015; Schoofs et al., 2021). To assess the fractionation efficiency and convertibility, the product streams were thoroughly characterized for chemical composition. In addition, the cellulose-rich pulps were enzymatically hydrolyzed to assess the cellulose accessibility. An emphasis is put on the lignin extracts which were subjected to detailed structural characterization, including gravimetric yield quantification, two-dimensional Heteronuclear Single Quantum Coherence Nuclear Magnetic Resonance (2D HSQC NMR) analysis, and profiling of LCCs.

By providing this detailed study including cell wall composition and lignin architecture as well as LCC profiling of different peatland derived biomasses, this study supports the development of regionally adapted paludiculture systems. Holistic biomass valorization strategies enhance the economic attractiveness of rewetted peatlands within the emerging circular bioeconomy.

TABLE 1 Plant material used for experiments, including harvest time, origin, and source.

Plant species	Time of harvest	Location	Provider
Giant miscanthus (*Miscanthus x giganteus*)	April-May 2023	Campus Klein Altendorf in North Rhine-Westphalia	University of Bonn
Common reed (*Phragmites australis*)	February 2024	Paludiculture pilot site in Mecklenburg-Western Pomerania	University of Greifswald
Sedge (*Carex* spp.)	August 2023	Paludiculture pilot site of ARGE Donaumoos in Bavaria (part of MOORuse project; Eickenscheidt et al., 2023)	University of Greifswald
Reed canary grass (*Phalaris arundinacea*)	August 2023	Paludiculture site from the Moorhofer Grünlandhof in Brandenburg	University of Greifswald

2 Materials and methods

2.1 Plant material

Dry aboveground biomass (hay) from three peatland grass species was used in this study. Giant Miscanthus served as a terrestrial reference species. All grasses were harvested from one field site each. As is typical for field-collected material, the hay may contain minor proportions of other plant species. The information about the sample's dominating plant species, time and location of harvest, and the respective providers are shown in Table 1.

For simplicity, the plant material samples examined in this study are referred to by their genus names. All materials were milled with a SM 200 cutting mill (Retsch, Haan, Germany) using a 0.5 mm sieve. This material was used for the OrganoCat fractionation. In preparation of the wet chemical analysis, all materials were additionally ground to a fine powder using a M 400 ball mill (Retsch, Haan, Germany) in a metal beaker (3 times 1 min at 30 s^{-1}).

2.2 Biomass fractionation with OrganoCat technology

The OrganoCat process was carried out in three independent technical replicates following the procedure described in Grande et al. (2019), Weidener et al. (2020), Martinez Diazet et al. (2023) with minor modifications:

A 25 mL high-pressure reactor was charged with 1 g of dry *Miscanthus*, 10 mL of an aqueous acid solution (0.7 M phosphoric acid as catalyst), and 10 mL of 2-methyltetrahydrofuran (2-MTHF). The mixture was heated to 140 °C under stirring (1,500 rpm) for 3 h. These conditions were chosen to balance efficient fractionation with low degradation. This approach has shown to be efficient in the separation of sugars, lignin, and cellulose-rich pulp while avoiding excessive formation of undesired degradation products (Weidener et al., 2021).

After cooling, the reaction mixture was transferred to a separation funnel to allow phase separation, during which lignin is extracted into the 2-MTHF, while the cellulose-rich pulp remained in the aqueous phase. The lignin extract was isolated from the reaction broth by centrifugation (10,000 rpm, 5 min, 20 °C), removed using a Pasteur pipette and transferred to a round-necked flask. The solvent 2-MTHF was evaporated in a rotary evaporator (40 °C, 15 min). All yields are given as wt% of the total biomass sample. Moisture and mineral content were not determined.

To synthesize sufficient lignin for HSQC-lignin analysis, a separate set of three OrganoCat replicates was conducted for each biomass. Procedure was the same as stated before until evaporation of the solvent 2-MTHF. For this set, after evaporation, the mass of remaining solid was determined. The complete solid of each replicate was then re-solubilized separately in 1 mL acetone and a sample of 300 µL was taken. Acetone was evaporated from the sample and the dry lignin samples were stored at room temperature for analysis.

Equation 1: Calculation of lignin extract yield (% of original biomass).

$$Lignin\,extract\,yield\,(\%\,original\,weight) = \frac{Weight\,of\,extracted\,lignin\,(mg)}{Initial\,biomass\,dry\,weight\,(mg)} \cdot 100 \quad (1)$$

For pulp yield, the pulp was dried in a drying-oven at 65 °C over night. The ratio of dried pulp and initial biomass weight was calculated.

Equation 2: Calculation of pulp yield (% of original biomass). The yield of pulp is expressed as the ratio of the oven-dried pulp mass after processing to the initial dry biomass mass.

$$Pulp\,yield\,(\%\,original\,weight) = \frac{Final\,pulp\,weight\,(mg)}{Initial\,biomass\,weight\,(mg)} \cdot 100 \quad (2)$$

The reported results represent the means and standard deviations of the three independent technical OrganoCat replicates.

2.3 Wet chemical characterization of plant material

Alcohol-insoluble residues (AIR) were obtained by sequential solvent extraction using 70% (v/v) ethanol, chloroform–methanol (1:1, v/v), and acetone to remove alcohol-soluble components. The resulting pellets were subjected to enzymatic starch removal using α-amylase and amyloglucosidase (Megazyme, Ireland), yielding

destarched AIR (dAIR). Following enzymatic digestion, the residues were washed repeatedly with deionized water and acetone, air-dried at room temperature. This dAIR was used as the standardized biomass material for all subsequent biomass composition analyses, which were all performed in three technical replicates. Each analysis method and replicate was performed using separate samples of the same dAIR material.

Crystalline cellulose was quantified following a modified Updegraff procedure. Non-crystalline and non-cellulosic polysaccharides were selectively removed using the acetic–nitric Updegraff reagent (Updegraff, 1969). The remaining cellulose-rich residues were subsequently hydrolyzed with 72% (w/v) sulfuric acid, and the released glucose was quantified by the anthrone spectrophotometric assay (Scott and Melvin, 1953).

Non-cellulosic polysaccharides in the dAIR were quantified by hydrolysis with trifluoroacetic acid (TFA) followed by monosaccharide separation using high-performance anion-exchange chromatography with pulsed amperometric detection (HPAEC-PAD), adapted from (Damm et al., 2017).

Lignin content was quantified using the acetyl bromide soluble lignin (ABSL) method (Foster et al., 2010a). Samples were treated with 25% (v/v) acetyl bromide and incubated at 50 °C for 3 h, followed by addition of 2 M NaOH, 0.5 M hydroxylammonium chloride, and glacial acetic acid to stabilize the reaction mixture. The solubilized lignin was then quantified spectrophotometrically by measuring absorbance at 280 nm. For calibration and to ensure comparability across analytical runs, a standard curve was prepared using Kraft lignin (Sigma-Aldrich, Seelze, Germany).

Total acetate content was quantified by saponifying the dAIR biomass with 0.5 M NaOH, followed by neutralization with 1 M HCl. The released acetate was subsequently determined enzymatically using the acetic acid assay kit (K-ACETRM, Megazyme, Ireland).

The reported results of the wet chemical characterization represent the means and standard deviations of the three technical replicates in each analysis.

2.4 Analyses of the OrganoCat fractions

2.4.1 Cellulose-rich pulp: composition analysis and saccharification

The same wet chemical analyses as described in chapter 2.3 were conducted on the cellulose-rich pulp obtained from the OrganoCat fractionation process. In this case, the dried pulp was used for the analyses, without prior AIR or dAIR pretreatment.

Enzymatic saccharification was performed with the untreated biomass and the OrganoCat pulps following established procedures with minor modifications (Damm et al., 2017). Saccharification of the untreated biomass (not dAIR) was performed in three technical replicates and the pulp of each of the OrganoCat triplicates was analyzed as technical replicates to obtain results of n = 3. The reported results represent the means and standard deviations.

For each reaction, 20 mg of dried material were suspended in 990 µL of 0.1 M citrate buffer (pH 4.5). Accellerase® 1,500 (60 FPU mL^{-1}, 82 CBU mL^{-1}, Genencor, Netherlands) was added at a volume of 10 µL per reaction. Avicel® cellulose served as an internal reference for cellulose hydrolysis efficiency. The suspensions were incubated in 1.5 mL reaction tubes and shaken at 50 °C for 72 h in an Eppendorf ThermoMixer Comfort. After incubation, enzymatic activity was terminated by heating the samples to 100 °C for 10 min. For the 0 h samples, the sample was heated to 100 °C before the enzyme was added to immediately inactivate the enzymes. The released glucose was quantified using the p-hydroxybenzoic acid hydrazide (PAHBAH) assay (Lever, 1972). The PAHBAH reagent was added to the supernatant and incubated for 10 min at 100 °C, then diluted with ultra-pure water after which absorbance was measured spectrophotometrically at 410 nm. All reactions were performed in triplicate. For eliminating any background absorption from the enzyme solution, the 0 h sample value was subtracted from the 72 h value. To determine the theoretically available glucose from glucan, both the glucose originating from cellulose and the glucose derived from hemicellulose were considered. The measured monosaccharides were converted into their corresponding anhydro-sugar equivalents using the appropriate conversion factors. Glucose released from cellulose was determined based on the glucan content of the biomass.

Equation 3: Calculation of the saccharification yield (η\etaη) based on the measured glucose released during enzymatic hydrolysis relative to the theoretical maximum glucose obtainable from the glucan fraction of the biomass. $M_{Glc,meas}$: Mass of measured, enzymatically released glucose. $M_{Gluc,theor}$: Mass of glucose that can theoretically be released from glucan.

$$\eta(\%) = \frac{m_{Glc,meas}}{m_{Gluc,theor}} \cdot 100 \quad (3)$$

2.4.2 Aqueous phase: hemicellulose composition analysis

The monosaccharide composition of the aqueous phase after OrganoCat was determined analogously to the non-cellulosic polysaccharides in the biomass, using high-performance anion-exchange chromatography with pulsed amperometric detection (HPAEC-PAD). The aqueous phase of each of the OrganoCat triplicates was analyzed as technical replicates to obtain results of n = 3. The reported results represent the means and standard deviations.

2.4.3 Lignin extract: carbohydrate and HSQC NMR analysis

Carbohydrate residues covalently linked to lignin were analyzed analogously to the non-cellulosic polysaccharides in the biomass, using TFA hydrolysis. The lignin extracts of the three OrganoCat replicates were pooled. The pooled samples were each measured three times and thus represent the compositional signature of lignin derived from the three OrganoCat extractions. The reported results represent the means and standard deviations. This analysis enables the determination of residual carbohydrates and LCCs in the solid lignin extract. Structural characterization of extracted lignin was conducted by ^{1}H–^{13}C HSQC NMR on a Bruker AVANCE 600 MHz NMR spectrometer with the Bruker standard pulse sequence “hsqcetgpsisp.2”. For this measurement, the lignin extract was prepared as described in chapter 2.2, and the obtained lignin

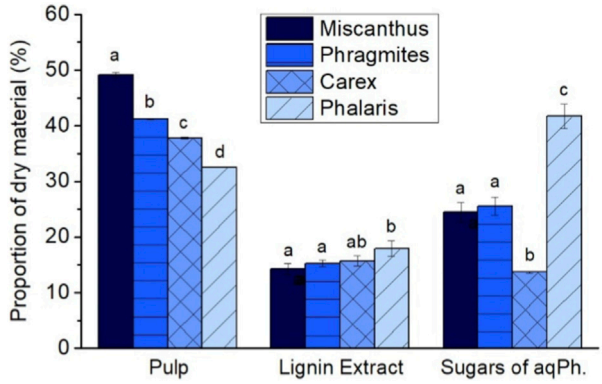

FIGURE 1
Gravimetric yields of cellulose-rich pulp and lignin extract, as well as total yield of TFA-hydrolyzed sugars in the aqueous phase (aqPh.). n = 3. Letters on columns indicate significance recording to Fisher LSD One-Way ANOVA.

samples were each dissolved in 0.5 mL DMSO-d6 and then measured. The solid lignin extract triplicates were analyzed as technical replicates to obtain results of n = 3. The reported results represent the means and standard deviations.

Spectra were recorded with a spectral width of 16 ppm (^{1}H) and 240 ppm (^{13}C), using 2048 (F2) and 256 (F1) data points, 128 scans, and a 1 s delay (total acquisition: 24 h). Chemical shifts were referenced to DMSO (δ_H = 2.50 ppm; δ_C = 39.52 ppm).

Signals of syringyl (S), guaiacyl (G), and p-hydroxyphenyl (H) units were assigned and quantified according (Schoofs et al., 2024) using:

$\sum (arom.) = \frac{S_{2,6}}{2+G_2} + \frac{H_{2,6}}{2}$ S%, G%, and H% were calculated relative to Σ(arom.).

Interunit linkages were quantified per 100 aromatic units. Their relative abundances were normalized to ∑(arom.), expressed as linkages per 100 aromatic units.

LCCs (phenyl glycoside (PG), benzyl ether (BE), and ester (Est) types) were identified via characteristic α-proton cross-peaks in the aliphatic region (Giummarella et al., 2016). Their relative abundances were normalized to Σ(arom.), expressed as linkages per 100 aromatic units (Giummarella et al., 2016).

2.5 Data analysis

To determine the content of the analyzed components in the untreated biomass, dilution factors and the weighed sample mass were considered to determine the mass fraction of the component in the sample material. In case of cellulose, the molar mass of glucose bound in cellulose was also considered in the calculation to calculate the cellulose content from the measured glucose concentration. The content of each component in the sample material was corrected by the dAIR yield to determine the content in the untreated biomass. All calculations were performed using Microsoft Excel.

Figure generation and statistical analyses were conducted using OriginPro 9. To assess the significance of differences in component contents across species, One-way ANOVA was performed on individual replicate values (n = 3 technical replicates per species), followed by Fisher's LSD post-hoc test for multiple comparisons (α = 0.05). Data are presented as mean ± standard deviation (n = 3). Statistical significance between samples is indicated in the figures by letters above the respective columns.

3 Results

3.1 OrganoCat biomass fractionation

OrganoCat fractionation resulted in pronounced, species-dependent differences in the recovery of cellulose-rich pulp, lignin extract of the organic phase, and hemicellulose-derived sugars in the aqueous phase (Figure 1). All peatland biomasses exhibited substantially lower pulp yields compared with *Miscanthus*, with reductions ranging from 16% to 33%. Among the peatland species, *Phragmites* showed the highest pulp recovery (41%) and *Phalaris* the lowest (33%).

The gravimetrically determined amounts of the lignin extract were comparable among species. *Miscanthus, Phragmites*, and *Carex* yielded similar amounts of lignin extract (14%–16%), in contrast, *Phalaris* exhibited a significantly increased lignin recovery (18%), producing approximately 28% more lignin extract than *Miscanthus*.

Species-specific differences were also observed in the hemicellulose-derived sugar yields recovered from the aqueous phase. *Carex* released significantly lower total sugar amounts (14%) compared with *Miscanthus* (24%), whereas *Phalaris* showed a significantly increased sugar yield (42%). Sugar recoveries from *Phragmites* were within the range observed for *Miscanthus* and did not differ significantly (26%).

3.2 Chemical composition of plant material and cellulose-rich pulp

The four grass species showed some differences in their chemical composition (Figure 2A). With about 40%, *Miscanthus* exhibited a significantly higher cellulose content than the peatland grasses. Among the latter, with about 30% *Phragmites* contained more cellulose than *Carex* and *Phalaris*, which showed comparable and significantly lower levels at about 25%. The contents of ABSL showed two distinct clusters: *Miscanthus* and *Phragmites* displayed comparable ABSL levels (around 25%), whereas *Carex* and *Phalaris* contained lower but mutually similar contents (around 18%). Hemicellulose amounts were comparable across all species and ranged from 20% to 25%. Acetylation levels remained below 5% in all biomasses, with *Miscanthus* and *Phragmites* showing the highest degrees of acetylation (3%–4%), followed by *Phalaris* (2%) and then *Carex* (1%). Overall, the compositional patterns revealed strong similarities between *Miscanthus* and *Phragmites*, and likewise between *Carex* and *Phalaris*, particularly with respect to cellulose and lignin.

The pulps derived from the biomasses displayed highly similar chemical profiles for all species, with the exception of a lower total sugar content in *Carex* (Figure 2B). The cellulose proportion was increased significantly to 56%–65% of the pulp, while the hemicellulose level was significantly decreased (to about 10%;

10.3389/fceng.2026.1799905

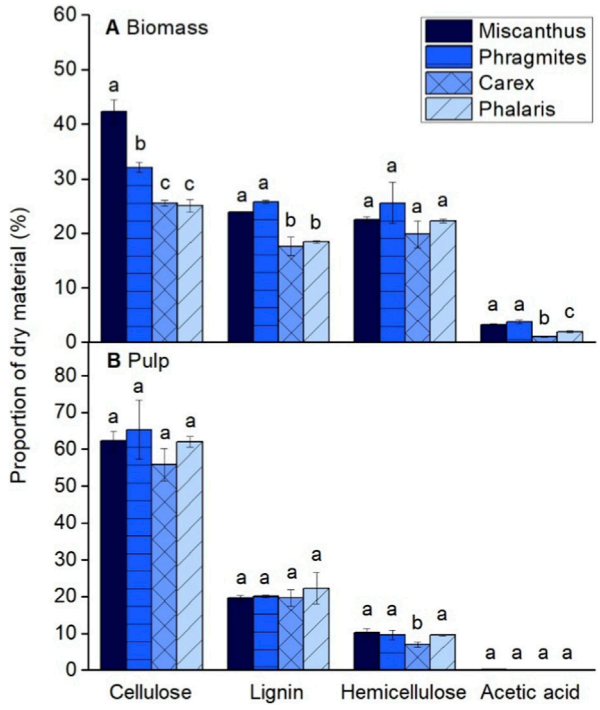

FIGURE 2
Chemical composition of the biomass **(A)** and the cellulose-rich pulp **(B)** contained from the OrganoCat fractionation process. Used methods: Seaman cellulose, ABSL, TFA hydrolysis of cell wall polysaccharides, Acetic acid kit. n = 3. Letters on columns indicate significance recording to Fisher LSD One-Way ANOVA.

Carex 7%) and acetic acid was completely absent. OrganoCat processing resulted in lignin extraction and thus a reduction of the absolute lignin content in the remaining pulp for all four investigated species, as evidenced by the recovery of lignin extract in the organic phase (Figure 1). For the relative ABSL contents (relative to dry material) in the cellulose-rich pulps however, a significant decrease was observed only for *Miscanthus* and *Phragmites*, whereas for *Carex* and *Phalaris* no statistically significant difference in the relative ABSL content compared to the untreated biomass was detected. In these latter species, lignin removal occurred in parallel with substantial losses of other cell wall components, particularly hemicelluloses. Consequently, the values of the ABSL content relative to the dry material may be the same for the resulting pulps (20%–22%) as for the native material despite a clear reduction in absolute lignin amount.

3.2.1 Enzymatic saccharification

The rate of enzymatic saccharification, which is calculated from the glucose released in the buffer and the total amount of glucan present in the substrate, differs substantially between untreated biomass and pulp (Figure 3). While the saccharification rate for biomass was around 15%, it was over 75% for pulp. Among the four biomasses, *Miscanthus* and *Phalaris* showed slightly higher saccharification rates (of 14%–20%) than the other two grasses (11%–13%), while in the pulp there were no significant differences between the species.

3.3 TFA-hydrolyzed sugar profiles of the biomasses before and after fractionation

Across all untreated biomasses, the hemicellulose-derived monomer profile was dominated by xylose (59%–76%), followed by substantial amounts of arabinose (11%–23%) and minor amounts (<10%) of galactose, glucose, mannose, and galacturonic acid (Figure 4A). *Miscanthus* and *Phragmites* contained slightly higher proportions of xylose (75%) and glucose (6%) than *Phalaris* and *Carex* (59%–64% xylose; 4% glucose), whereas the latter exhibited elevated levels of arabinose (22%) and galactose (6%) compared to *Miscanthus* and *Phragmites* (12% arabinose, 2% galactose).

Following OrganoCat-fractionation, the cellulose-rich pulps of all species showed a similar sugar composition in the TFA-soluble fraction (Figure 4B), with glucose as the predominant monomer (82%–87%), accompanied by smaller amounts of xylose (9%–15%). Arabinose was nearly absent (<3%), galactose was no longer detectable, and mannose persisted only in *Phalaris* (5%). Among the pulps, *Carex* contained the lowest total hemicellulose content (7% vs. 10%) but the highest relative glucose proportion (87%), whereas *Phragmites* exhibited the highest xylose proportion (15%).

In the aqueous phase, representing the OrganoCat-solubilized hemicellulose fraction, species-specific differences were most pronounced (Figure 4C), particularly in xylose, glucose, arabinose, and galactose. *Miscanthus* and *Phragmites* showed similarly high xylose levels (70%), whereas *Carex* exhibited substantially lower proportions (49%) and *Phalaris* the lowest (25%). The opposite trend was observed for arabinose (10%, 17%, 24%), galactose (3%, 9%, 15%), and glucose (11%–12%, 19%, 28%), which increased from *Miscanthus* and *Phragmites* toward *Carex* and *Phalaris*.

The residual sugars associated with the lignin extract also differed substantially between species (Figure 4D). In *Miscanthus*, the hydrolysates contained almost exclusively arabinose (69%) and xylose (22%), despite xylose being the dominant sugar in the raw biomass of all species. In contrast, lignin extracts of *Carex* and *Phalaris* released arabinose, galactose, glucose, and xylose in comparable proportions, deviating markedly from their native carbohydrate profiles. *Phragmites* exhibited a pattern most similar to *Miscanthus*, though with roughly half the arabinose content and nearly twice the glucose content. These results demonstrate that the composition of lignin-bound polysaccharides varies substantially among the investigated grasses. Despite these differences, the total amount of sugars released after TFA hydrolysis of the lignin extract was comparable across all species (0.6%–0.8%).

3.4 Characterization of lignin extracts

Analysis of lignin structures by 2D HSQC NMR revealed differences between *Miscanthus* and the three peatland biomasses (Figure 5). The abundance of β–*O*–4 linkages was similar among *Miscanthus*, *Phragmites*, and *Carex* (16%–19%), whereas *Phalaris* showed a reduction of almost 34% relative to *Miscanthus*. In parallel, *Carex* and *Phalaris* exhibited lower proportions of both β–β- (1%–2%) and β–5-bonds (3%–4%), whereas these were above 3% and 5%, respectively, in the other species. The monolignol composition differed between species: the G-lignin content in *Phalaris* was up to 20% higher than in *Miscanthus*. *Carex* and *Phragmites* also exhibited a slightly higher G-lignin

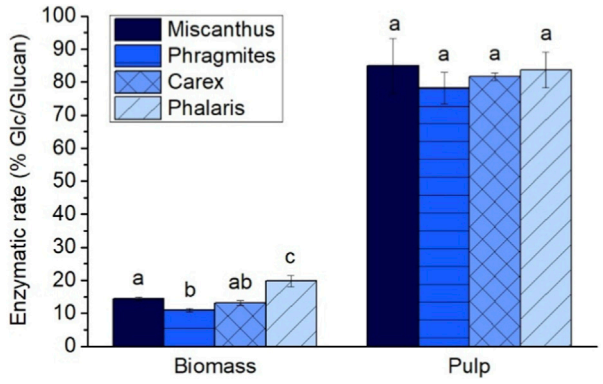

FIGURE 3
Enzymatic saccharification rate after 72 h of treating the substrates with Accellerase 1,500. n = 3, except Carex pulp: n = 2. Letters on columns indicate significance recording to Fisher LSD One-Way ANOVA.

content (2%–4% higher) compared to *Miscanthus*. Furthermore, all three peatland grasses had an S-lignin content that was up to 28% lower than that of *Miscanthus*. This results in a lower S/G ratio for all peatland grasses.

Despite these structural differences, the overall signal intensity of the HSQC spectra for the peatland biomasses remained significantly lower compared to *Miscanthus*, indicating a generally reduced abundance or detectability of aromatic lignin units in the extracted fractions.

Representative spectra from the LCC analysis and the molecular structure of LCCs are shown in Figure 6. Chemical features derived from LCC analysis also demonstrated consistent species-specific trends (Figure 6). The number of LCC bonds was approx. 25% higher in *Carex* (55%) and *Phalaris* (49%) than in *Miscanthus* (44%), with ester bonds (Est) in particular increasing by up to 53% compared to *Miscanthus*. Despite these differences, the overall amount of sugars released after TFA hydrolysis of the lignin extract was comparable across all species (0.6%–0.8%). This suggests a similar overall quantity of polysaccharides associated with the lignin extract. Nevertheless, the composition of lignin-bound polysaccharides varies substantially among the investigated grasses (Figure 4). However, *Carex* exhibited significantly higher (13%) and *Phalaris* significantly lower ferulate contents than *Miscanthus* (9%).

4 Discussion

4.1 Peatland grasses show clear differences in their OrganoCat fractionation

The OrganoCat fractionation results reveal distinct processing behaviors between *Miscanthus* and the peatland grasses. All peatland species produced lower pulp yields than *Miscanthus* (Figure 1), indicating a more extensive dissolution of structural components under OrganoCat conditions. Similar reductions in pulp recovery have been reported for grass biomasses with easily hydrolizable matrix domains and heightened susceptibility to acid-catalyzed hydrolysis (Bergs et al., 2021; Chu et al., 2021). The lower pulp retention might suggest that the peatland grasses are less recalcitrant to the applied process configurations (Grande et al., 2015; Grande et al., 2019). Furthermore, the cellulose content in the untreated peatland biomasses was lower than in *Miscanthus*, which limits the maximum expected pulp yield, as less cellulose is available for retention in the solid pulp fraction (Figure 2A).

The amounts of lignin extract obtained after OrganoCat fractionation were broadly comparable across species, with the notable exception of *Phalaris*, which exhibited an approximately 20% higher gravimetric yield of lignin extract than *Miscanthus* (Figure 1). Interestingly, this elevated lignin extraction contrasts with the lower ABSL content determined for *Phalaris* in the untreated biomass (Figure 2A), while both, the ABSL content of the resulting pulp (Figure 2B) and the gravimetric mass of the lignin extract, were comparably high. The higher apparent lignin extract yield might therefore partly reflect the co-extraction of non-lignin extractives that contribute to the yield and inflate the apparent lignin recovery. At the same time, the slightly elevated ABSL content remaining in the *Phalaris* pulp might suggest a less efficient lignin removal during OrganoCat fractionation, which could be associated with a more condensed lignin structure that is less susceptible to extraction. Such effects have been reported for grass biomasses where lignin condensation limits delignification efficiency despite moderate native lignin contents (Tarasov et al., 2018). The comparable lignin extract recoveries observed for *Miscanthus*, *Phragmites*, and *Carex* are consistent with previous studies finding that *Phragmites* lignins show a similar extractability using OrganoCat despite differences in the lignin´s structure and composition (Grande et al., 2015).

Sugar yields of the aqueous phase showed a strong species-dependent divergence, even though the untreated biomasses showed rather similar contents of hemicelluloses (Figure 2A). *Carex* released significantly fewer sugars into the aqueous phase than *Miscanthus* (Figure 1), indicating restricted hydrolysis or solubilization of its polysaccharide fraction. Limited sugar release under OrganoCat has been linked to reduced carbohydrate accessibility or hemicellulose structures that are less responsive to acid-catalyzed cleavage (Grande et al., 2019). Among the studied species, *Carex* exhibited the highest abundance of LCC-signals, which could have restricted hemicellulose release. Its potentially higher proportion of highly substituted arabinoxylans might not have been completely solubilized under the applied OrganoCat conditions. Additional studies are required to elucidate the underlying mechanisms of this observation. In contrast, *Phalaris* produced a significantly higher sugar yield than *Miscanthus*, consistent with studies demonstrating that increased lignin removal enhances solvent penetration and improves acid-catalyzed polysaccharide depolymerization in the OrganoCat system (Weidener et al., 2020). The sugar yield of *Phragmites* did not significantly differ from *Miscanthus*, which might suggest a similar accessibility.

In the OrganoCat fractionation yield balances, *Carex* displayed a notable discrepancy in its overall recovery: the sum of cellulose-rich pulp, lignin extract, and hemicellulose sugars of the aqueous-phase remained significantly below 100% (Figure 1). This discrepancy is likely linked to the specific biomass composition of sedge-type peatland species, which are known to contain comparatively high proportions of lipophilic extractives (waxes, fats, phenolic compounds) and mineral ash that are not accounted for in standard lignocellulosic fractionations (Janyszek-Sołtysiak et al.,

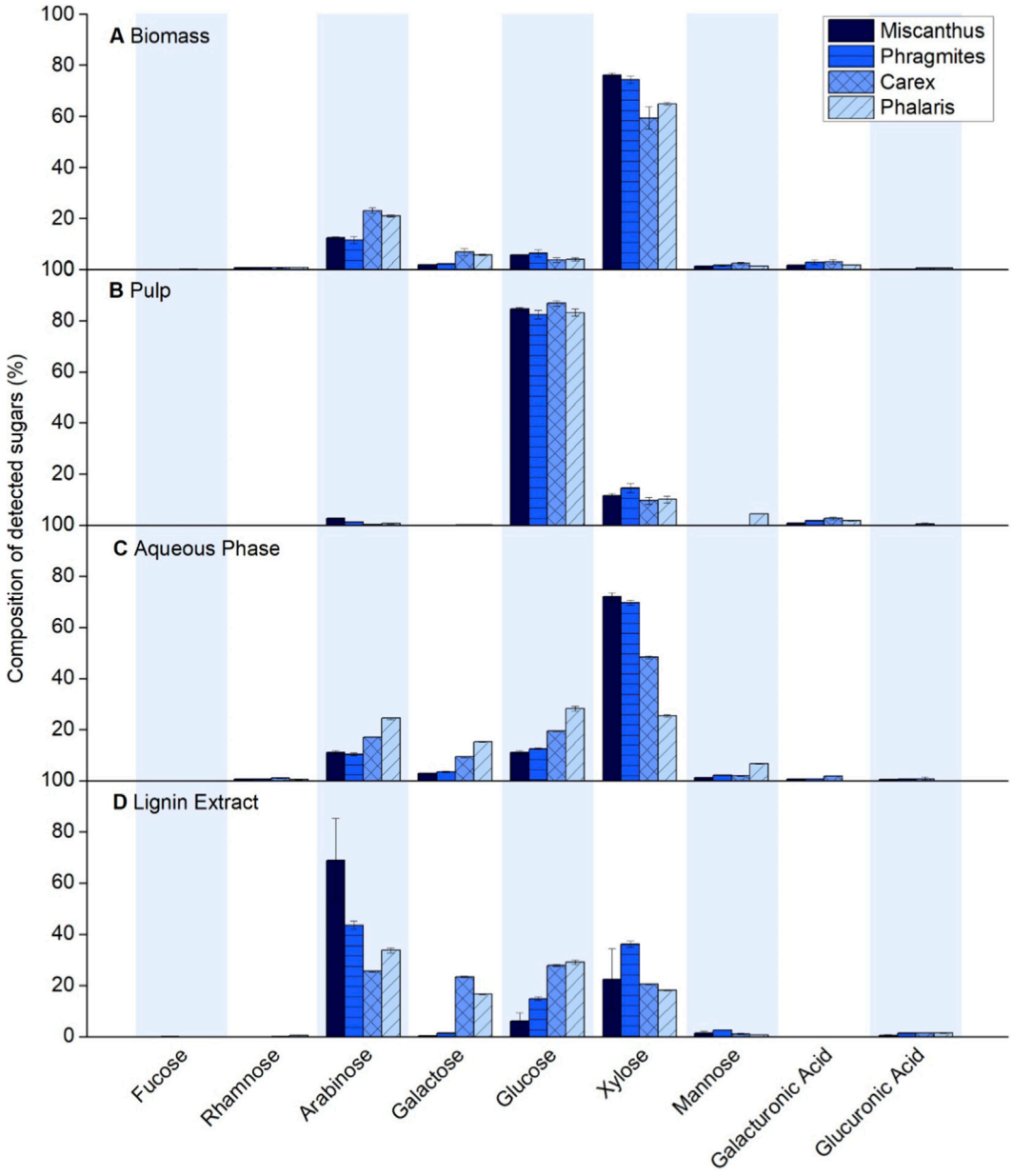

FIGURE 4
Composition of TFA-hydrolyzed sugars of the four analyzed biomasses **(A)** and their three fractions after chemical fractionation: the cellulose-rich pulp **(B)**, the sugars in the aqueous phase **(C)** and the lignin extracted in the organic phase **(D)**. n = 3. The determination of the sugars from the lignin extract was conducted in triplicates from one pooled sample of the triplicates of the OrganoCat, therefore no ANOVA was performed.

2021). However, higher contents of extractives and minerals can also be expected for the other peatland grasses, given that comparable amounts of alcohol-soluble compounds were removed during pretreatment of all peatland biomass samples (see Table A1). Yet only *Carex* exhibited a pronounced yield gap compared to *Miscanthus*.

4.2 Peatland grass pulps show similar properties despite initial biomass differences

High cellulose and lignin contents are functionally linked to the mechanical stability required in tall grasses like *Miscanthus* and *Phragmites*, where dense sclerenchyma tissue supports large culms exposed to wind or fluctuating water levels. The compositional differences observed among *Miscanthus*, *Phragmites*, *Phalaris*, and *Carex* thus might reflect potential functional adaptations to their respective growth forms (Figure 2A). In our study, *Miscanthus* and *Phragmites* showed higher cellulose (42%, 32%) and ABSL contents (24%, 26%) than *Phalaris* and *Carex* (25% cellulose, 18% ABSL). The detected values align with prior composition studies: Gismatulina et al. (2022) reported cellulose levels of 43%–56% in *Miscanthus x giganteus* cultivated in different climate regions and lignin contents of 17%–25%, characteristic of tall perennial C4 grasses with thick structural culms. *Phragmites*

10.3389/fceng.2026.1799905

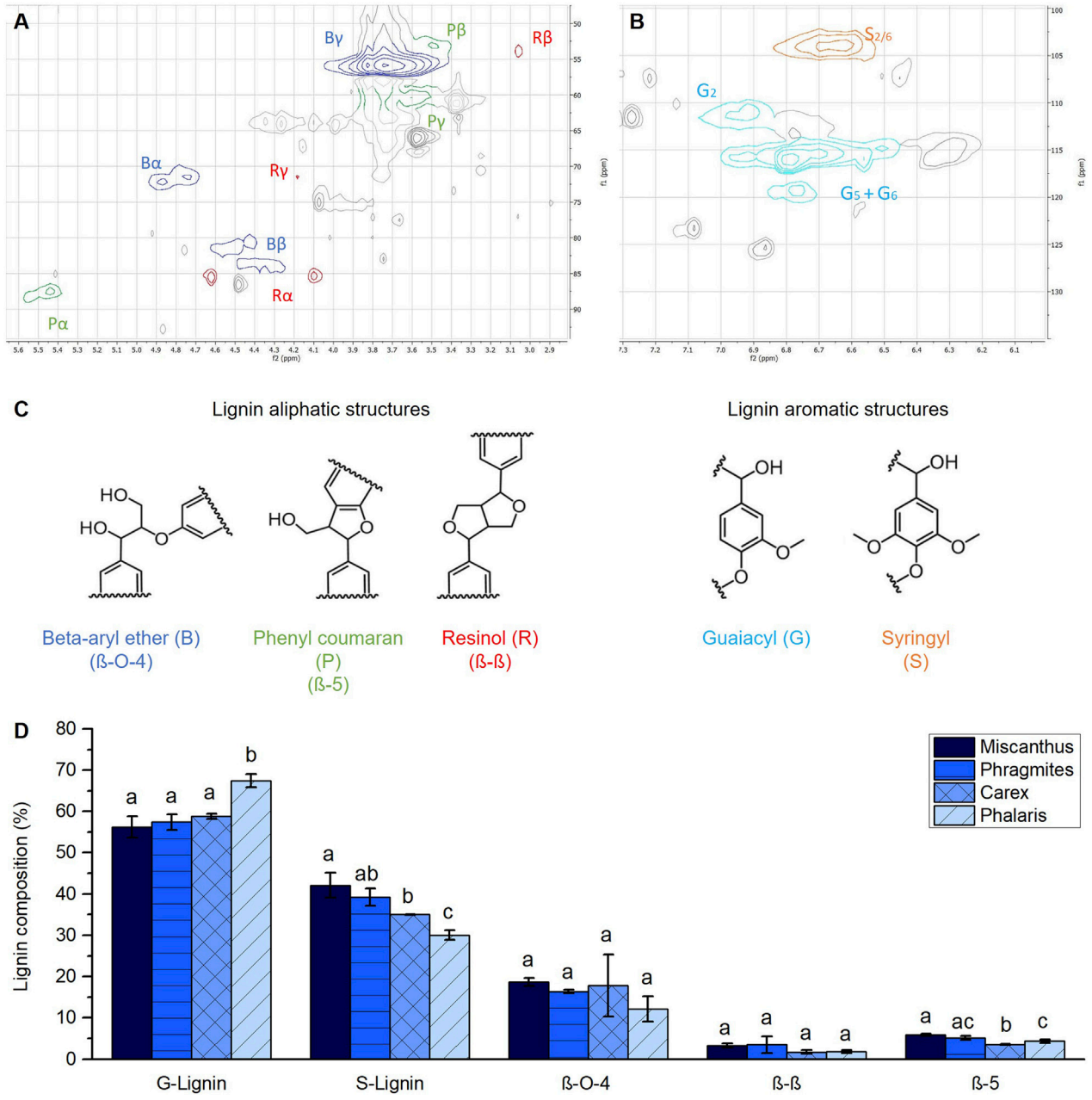

FIGURE 5
Representative 2D-HSQC spectrum of Miscanthus x giganteus lignin showing the regions of **(A)** lignin linkages, **(B)** lignin monomer units, **(C)** chemicals structures and **(D)** lignin monomer composition and linkages per 100 monomer units of all investigated species. Lignin aliphatic region: δ_H = 3.0–5.6 ppm, δ_C = 50–90 ppm. Lignin aromatic region: δ_H = 6.4–7.1 ppm, δ_C = 100–140 ppm. n = 3. Letters on columns indicate significance recording to Fisher LSD One-Way ANOVA.

australis stems were reported to contain 35%–37% cellulose and about 6% lignin (Rodriguez-Dominguez et al., 2022). ABSL levels of *Phragmites* were considerably higher in our study, which could be due to the different method (NREL 42618) applied by Rodriguez-Dominguez *et al.*, known to give lower values than the ABSL method. In contrast, *Phalaris arundinacea*, a temperate C3 grass of the Pooideae, and most *Carex* species (Cyperaceae) develop more leaf-rich, herbaceous canopies with thinner stems. Studies on *Phalaris* show cellulose contents of about 30%–37%, thus considerably higher than in this study but still lower than in *Miscanthus*, and lignin contents of around 14%–23%, aligning the results presented here (Strašil et al., 2005; Aysu, 2012). The chemical composition of sedges can vary broadly between species as has been shown in a study analyzing 9 different sedge species resulting in cellulose contents from 30%–46% and lignin contents from 12%–28% (Waliszewska et al., 2013), which is also comparable to the composition of *Phalaris* and lower than the contents in *Miscanthus*. Thus, the compositional similarity of *Phalaris* and

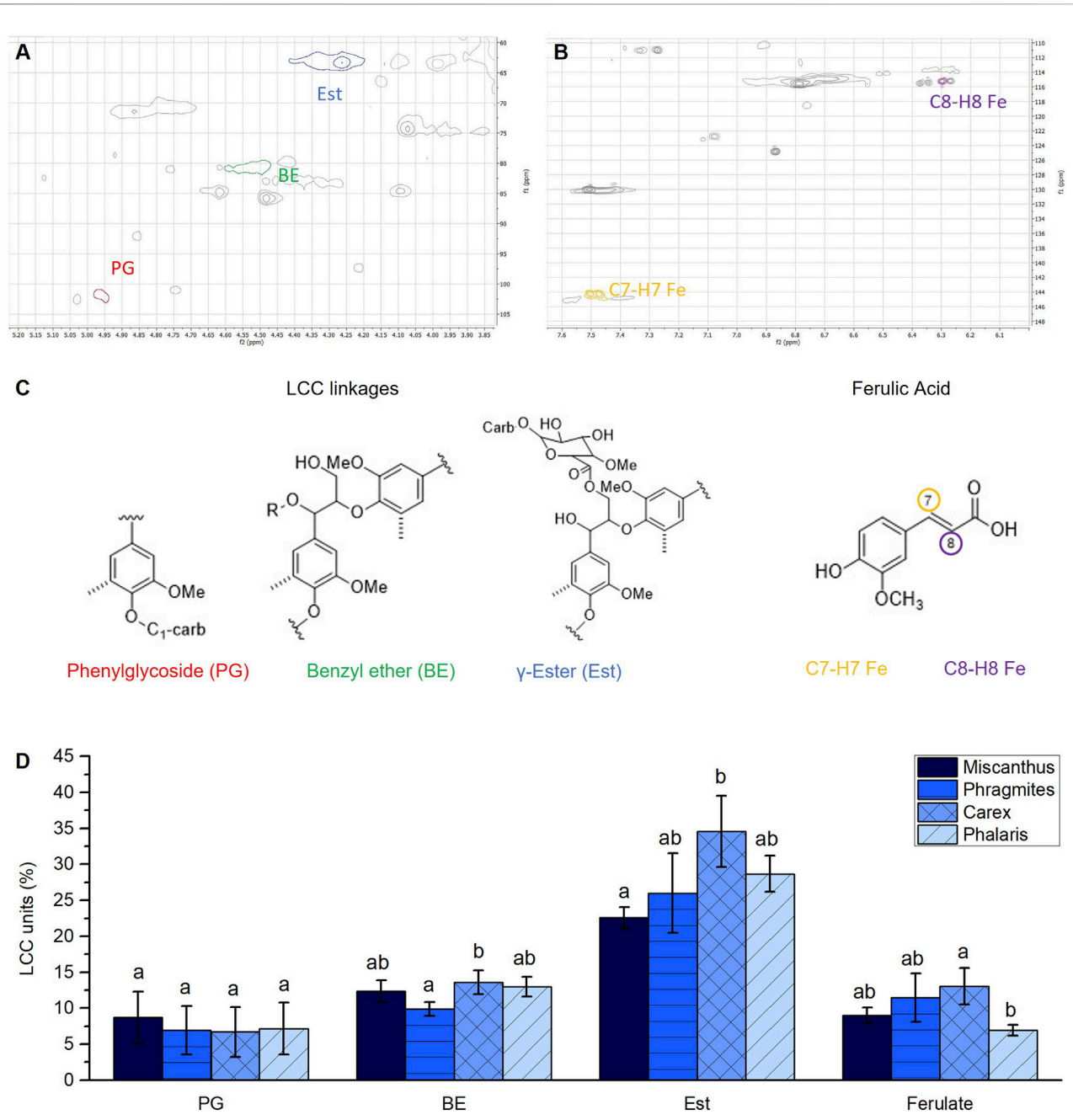

FIGURE 6
Representative 2D-HSQC spectrum of Miscanthus x giganteus lignin showing the regions of **(A)** examined LCC linkages and **(B)** ferulates, **(C)** the chemical structures of examined LCC linkages and ferulates and **(D)** LCC unit proportions. LCC linkages region: δ_H = 4.2–5.1 ppm, δ_C = 60–105 ppm. Ferulic Acid region: δ_H = 6.2–7.6 ppm, δ_C = 120–150 ppm. To determine LCC units and LCC proportions, the peaks of 2D HSQC NMR of extracted lignin were normalized per 100 HGS monomer units. The contents of ferulates were normalized to the sum of HGS monomer units. n = 3. Letters on columns indicate significance recording to Fisher LSD One-Way ANOVA.

Carex with lower cellulose and lignin levels, despite belonging to different phylogenetic families, could indicate that growth form and ecological factors play an important role in lignocellulosic composition. Nevertheless, all four investigated plants share the classical commelinoid monocot "type II" cell wall (Vogel, 2008), explaining the broadly similar hemicellulose levels (Figure 2A) and composition observed (Figure 3A).

All four plant species produced pulps with very similar cellulose, hemicellulose and residual ABSL proportions (Figure 2B), meaning that even species with initially lower cellulose content, such as *Carex* or *Phalaris,* yield pulps comparable in composition to those from *Miscanthus* or *Phragmites*. This can be advantageous for later valorization since compositional variation could have less consequences during the processing. This may widen the usable feedstock spectrum in paludiculture-based value chains and suggest that mixed-species harvests, common in rewetted peatlands, could be co-processed without substantial loss of product uniformity. For peatland management, where species composition can vary spatially

and temporally, such robustness in processing has the potential to reduce logistical constraints and enhance economic feasibility.

The relatively high residual ABSL content detected in the pulps might be partly explained by the strong relative enrichment effects caused by hemicellulose loss. It also might be influenced by structural accessibility of lignin, which plays a major role in OrganoCat delignification efficiency (Schoofs et al., 2024). The remaining lignin in the pulp shows that a fraction of lignin remained inaccessible to the OrganoCat solvent system. This might be due to cell-wall architectural barriers or stronger lignin–carbohydrate linkages; solubility and aggregation of certain lignin domains may also contribute (see chapter 4.5).

Enzymatic saccharification was included as an indicator for cellulose accessibility and metric of the biomass's suitability for biochemical conversion pathways. Results are presented as the saccharification rate, meaning how much of the glucan available in the substrates has been hydrolyzed into glucose. A clear distinction emerged between the enzymatic digestibility of the native biomasses and their corresponding pulps (Figure 3). Saccharification rates of the pulps were almost 6-fold higher compared to the untreated biomasses, indicating that the fractionation process reduced cell wall recalcitrance. The removal of hemicellulose and part of the lignin matrix is known to increase cellulose accessibility by disrupting the physical shielding of microfibrils and reducing nonproductive binding of enzymes to lignin (Zhao et al., 2012). Furthermore, saccharification rates among the pulps of all three peatland species and *Miscanthus* showed a close similarity. This is consistent with the previously discussed convergence in cellulose content after fractionation. It has been reported that pretreatment severity, rather than feedstock identity, becomes the dominant determinant of hydrolysability once cellulose purity surpasses a threshold at which enzyme accessibility is no longer limited by matrix polysaccharides or lignin (Li et al., 2022). Consequently, the cellulose isolated from peatland grasses exhibits saccharification rates comparable to that of an established reference crop such as *Miscanthus*, underscoring the technical suitability of wetland biomass for sugar-based bioconversion pathways.

4.3 Substitution of arabinoxylan divides the peatland grasses

Across all four plant materials a typical grass-type hemicellulose signature was observed in the untreated biomass (Figure 4A). As mentioned before, all plants investigated share the classical commelinoid monocot "type II" cell wall, known to be composed of cellulose fibers encased mainly in glucuronoarabinoxylans (Vogel, 2008). We could confirm the reported high xylose and low arabinose values for *Miscanthus* (Schäfer et al., 2019) and *Phragmites* (Zhang et al., 2018) indicating low-substituted arabinoxylans as the predominant hemicellulose in those species. *Phalaris* and *Carex* displayed elevated arabinose and galactose levels, indicating more highly substituted arabinoxylans, which likely reflect developmental factors rather than fundamental structural divergence. Research indicates that juvenile grass tissues contain more highly substituted arabinoxylans, whereas branching decreases with maturation (Suzuki et al., 2000; Fincher, 2009). Since both, *Carex* and *Phalaris,* were harvested in August while *Phragmites* and *Miscanthus* were harvested after the winter, the distinct profile plausibly results from a lower degree of maturation.

Marked shifts in sugar composition were observed after fractionation (Figure 4B). As to be expected, the cellulose-rich pulps contained predominantly glucose (>80% of the detected sugars) and only minor traces of other carbohydrates (<1.5% of the dry material) in the TFA hydrolysate, demonstrating a significant reduction in hemicelluloses, as the biomass prior to the fractionation contained 19%–25% non-glucose carbohydrates. The glucose-dominant profile indicates that the pretreated (rather the amorphous, not the crystalline) cellulose fraction was partially hydrolyzed by TFA in the analysis (Foster et al., 2010b). The hemicellulose-rich aqueous phase of all plant species retained the pattern of the biomass sugar composition but with slightly elevated glucose levels (Figure 4C), which might indicate the co-extraction of non-cellulosic glucans such as starch or mixed-linkage (1→3,1→4)-β-d-glucans, which are characteristic hemicellulosic components of grass cell walls and are readily hydrolyzed under mild acidic conditions (Fry et al., 2008; Grande et al., 2019). Although the sugar profiles of *Carex* and *Phalaris* were very similar in biomass, pulp and lignin extract, they showed pronounced differences in the aqueous phase: the pattern of lower xylose and higher arabinose, glucose and galactose contents compared to *Miscanthus* and *Phragmites* was notably more pronounced in *Phalaris* than *Carex*. This supports the aforementioned assumption that those species possess more highly arabinose-substituted glucuronoarabinoxylans. Carbohydrate residues were also detected in the lignin extract (Figure 4D), indicating the presence of lignin–carbohydrate complexes (see chapter 4.4), but in very little amounts (<1% of dry material).

4.4 Peatland grasses exhibit structurally reinforced lignin

The peatland grasses all had lower S-type lignin proportions than *Miscanthus*, while the G-type lignin proportion of *Carex* was markedly higher. The β–O–4 bonds were comparable to those in *Miscanthus*, accompanied by a lower proportion of β–β and β–5 couplings in *Carex* and *Phalaris* (Figure 5). This shift toward G-rich, C–C-bonded structures is characteristic of more condensed lignin matrices and aligns with lignin formed under oxidative or stress-prone conditions (Ralph et al., 2004). The particularly high condensation degree observed might correspond with its ecological niche, where reinforced cell walls, microbial resistance, and hydrophobicity are critical for survival in periodically anoxic and waterlogged environments. Such condensed architectures have repeatedly been associated with mechanical strengthening and reduced degradability in stress-adapted grasses (Ralph et al., 2004; Vanholme et al., 2010). *Miscanthus* exhibited a higher arabinose content in the lignin extract (Figure 4D), indicating a predominant reliance on ferulate-mediated arabinoxylan–lignin cross-linking, in which arabinose residues serve as anchoring points for covalent integration of hemicelluloses into the lignin network. In contrast, the peatland grasses displayed a notably higher overall abundance of LCCs, particularly ester-type linkages (Figure 6). This distinction reflects fundamental differences in cell wall architecture: while *Miscanthus* utilizes targeted

feruloylated arabinoxylans to establish specific lignin-hemicellulose bridges, peatland species rely on a broader spectrum of LCC chemistries, leading to extensive cross-linking without selective arabinose enrichment. Such ferulate-mediated cross-linking strategies are well established in grass cell walls, where they contribute to structural rigidity and controlled matrix assembly (Vanholme et al., 2010; Hatfield et al., 2017; Terrett and Dupree, 2019).

However, despite this higher LCC density, HSQC NMR revealed substantially lower ferulate signal intensities in *Phalaris* (Figure 6). At first glance, this appears contradictory; yet the mechanistic basis of ferulate incorporation resolves the discrepancy. This is consistent with previous studies showing that ferulate-containing ester LCCs rapidly lose their diagnostic vinylic HSQC signals upon radical coupling, becoming spectroscopically masked within the lignin matrix (Lawoko et al., 2005; Giummarella et al., 2016).

The TFA-hydrolysable carbohydrate profiles of the lignin extracts further reveal species-specific differences in LCC composition (Figure 4D), aligning with the differences in general hemicellulose composition discussed in chapter 4.3. *Miscanthus* lignin extract released almost exclusively arabinose and xylose, consistent with the dominance of feruloylated arabinoxylans as the major LCC-forming hemicellulose in grasses (Ralph et al., 2004; Giummarella et al., 2016). *Carex* and *Phalaris* yielded a more heterogeneous mixture of arabinose, galactose, glucose, and xylose in similar proportions, indicating potential involvement of diverse polysaccharides, such as pectic arabinans/galactans and mixed-linkage β-glucans, in LCC formation. Such structural flexibility is characteristic of wetland grasses with adaptive cell wall remodeling under fluctuating hydrological stress (Schellekens et al., 2012). *Phragmites* displayed a profile closest to *Miscanthus* but with markedly reduced arabinose and elevated glucose, a pattern compatible with condensed lignin matrices in which glucan-derived LCCs or tightly associated cellulose–lignin domains become more prevalent (Balakshin et al., 2011).

Despite differences in LCC density and composition, all species released similar total sugar quantities after TFA hydrolysis of the lignin extract (compare Figure 4). This suggests that peatland grasses might possess either (i) shorter polysaccharide chains attached to lignin or (ii) that these chains are sterically shielded within more condensed lignin domains, limiting hydrolytic accessibility. The latter interpretation aligns closely with the reduced S/G-ratio and increased C–C coupling observed in the peatland species. Mechanistic studies have shown that lignin condensation and ferulate-mediated cross-linking reduce polysaccharide mobility, restrict solvation, and hinder cleavage of xylan–ester linkages (Tarasov et al., 2018; Giummarella et al., 2019). These phenomena provide a possible direct and coherent explanation for the comparable sugar yields across species despite markedly different LCC architectures.

Overall, the combined structural, spectroscopic, and hydrolytic evidence demonstrates that peatland grasses develop highly condensed, cross-linked lignin matrices enriched in chemically transformed ferulate-derived LCCs. These architectures might be part of adaptive strategies to the hydrological and microbial pressures of peatland environments, contrasting with the more linear, arabinoxylan-dominated LCC networks of *Miscanthus*.

5 Conclusion

The pulp yields of *Phragmites australis* (41%), *Phalaris arundinacea* (33%), and *Carex* spp. (38%) were lower than those of *Miscanthus x giganteus* (49%), reflecting their naturally lower cellulose content compared to high-performing C4 crops and indicating a more extensive dissolution of structural components. Nevertheless, the consistently high saccharification efficiencies around 75% indicate that cellulose quality and enzymatic accessibility are fully retained once isolated. Those yield differences should be interpreted within the broader sustainability perspective of paludiculture, where biomass production serves as one component of a multifunctional system that delivers additional benefits such as peat conservation, greenhouse gas mitigation, water regulation, and habitat protection. Within this context, even moderate yields may represent a valuable contribution to regional bio-based value chains, particularly when lignin and hemicellulose co-products are also valorized.

Distinct hemicellulose profiles further reveal the biochemical diversity of the studied species. *Miscanthus* and *Phragmites* hemicellulose was dominated by xylose and arabinose from arabinoxylans, whereas *Carex* and *Phalaris* exhibited more complex mixtures of xylose, arabinose, galactose, and glucose, indicative of more highly substituted arabinoxylans or multiple polysaccharide classes such as pectins and mixed-linkage glucans. These compositional differences could create opportunities for tailored valorization routes from pentose fermentation and catalytic upgrading to specialty-sugar production. At molecular level, peatland grasses contain lignins that are denser and more cross-linked than those of *Miscanthus*. The LCC content in peatland grasses was up to 25% higher than in *Miscanthus*. The ferulate content was lower in *Phalaris* (7% compared with 9%). In *Phalaris*, an increased frequency of guaiacyl units (20% higher than in *Miscanthus*), reduced ß-ß (1.8% versus 3.3%) and reduced ß-5-linkages (4.4% versus 5.8%), as well as higher densities of lignin-carbohydrate complexes, characterize their lignin architectures. It was also demonstrated that the composition of lignin-bound polysaccharides varies substantially among the investigated grasses.

Such structural features may be consistent with adaptation to waterlogged and microbially challenging environments, where durability offers ecological advantages. In contrast, *Miscanthus* retains a more linear lignin network with detectable ferulate content, explaining its lower recalcitrance.

This study demonstrates that OrganoCat pretreatment can overcome species-specific recalcitrance among the four grasses. Despite clear differences in biomass composition, hemicellulose profiles, and lignin architectures, the process produced cellulose-rich pulps with comparable composition and saccharification efficiencies across all species. This shows that the applied pulping has decreased the interspecific variability in cellulose accessibility, creating more homogeneous feedstock streams for cellulose application. Consequently, cellulose isolated from rewetted peatland biomass matches the convertibility of *Miscanthus* × *giganteus*, confirming its technical feasibility for bio-based product formation.

Overall, the results highlight the valorization potential of rewetted peatland biomass. Its compositional diversity combined with the high biochemical uniformity of the resulting pulps and its multifunctional sustainability benefits make paludibiomass a

promising and regionally available feedstock for climate-friendly and circular bioeconomy value chains. By aligning technological development with ecological and socio-economic benefits, future research can advance the full potential of rewetted peatland biomass, transforming it from an emerging niche resource into a cornerstone of regional, climate-adaptive bioeconomy strategies.

Data availability statement

The raw data supporting the conclusions of this article will be made available by the authors, without undue reservation.

Author contributions

KU: Conceptualization, Resources, Methodology, Investigation, Data Curation, Formal Analysis, Visualization, Writing – original draft, Writing – review and editing. JR: Conceptualization, Methodology, Investigation, Data Curation, Formal Analysis, Visualization, Writing – original draft, Writing – review and editing. MH: Investigation, Data Curation, Writing – review and editing. PG: Conceptualization, Supervision, Writing – review and editing. HK: Conceptualization, Funding acquisition, Resources, Supervision, Writing – review and editing.

Funding

The author(s) declared that financial support was received for this work and/or its publication. This research was largely done within the BioSC project "OptiCellu". The scientific activities of the Bioeconomy Science Center were financially supported by the Ministry of Culture and Science within the framework of the NRW Strategieprojekt BioSC (No. 005-2012-0107).

Acknowledgements

The authors would like to thank Dr. Michael Rühs (University of Greifswald) for providing the peatland biomasses and Prof. Dr. Ralf Pude (University of Bonn) for providing the *Miscanthus* material. Furthermore, we would like to thank Dagmar Drobietz and Benedict Ohrem for their support in carrying out the experiment.

Conflict of interest

The author(s) declared that this work was conducted in the absence of any commercial or financial relationships that could be construed as a potential conflict of interest.

Generative AI statement

The author(s) declared that generative AI was not used in the creation of this manuscript.

Any alternative text (alt text) provided alongside figures in this article has been generated by Frontiers with the support of artificial intelligence and reasonable efforts have been made to ensure accuracy, including review by the authors wherever possible. If you identify any issues, please contact us.

Publisher's note

References

Abel, S., and Kallweit, T. (2022). "Potential paludiculture plants of the holarctic," in *Proceedings of the Greifswald Mire Centre, 04*, 440.

Aysu, T. (2012). Supercritical fluid extraction of reed canary grass (Phalaris arundinacea). *JBB* 41, 139–144. doi:10.1016/j.biombioe.2012.02.024

Balakshin, M., Capanema, E., Gracz, H., Chang, H. m., and Jameel, H. (2011). Quantification of lignin–carbohydrate linkages with high-resolution NMR spectroscopy. *Planta* 233 (6), 1097–1110. doi:10.1007/s00425-011-1359-2

Bergs, M., Monakhova, Y., Diehl, B. W., Konow, C., Völkering, G., Pude, R., et al. (2021). Lignins isolated *via* catalyst-free organosolv pulping from miscanthus x giganteus M. sinensis, M. robustus and M. nagara: a comparative study. *Molecules* 26 (4), 842. doi:10.3390/molecules26040842

Böll-Stiftung, H. (2023). *Peatland Atlas 2023: Facts and Figures About Wet Climate Guardians*.

Bonn, A., Reed, M. S., Evans, C. D., Joosten, H., Bain, C., Farmer, J., et al. (2014). Investing in nature: developing ecosystem service markets for peatland restoration. *Ecosyst. Serv.* 9, 54–65. doi:10.1016/j.ecoser.2014.06.011

Brienza, F., Cannella, D., Montesdeoca, D., Cybulska, I., and Debecker, D. P. (2024). A guide to lignin valorization in biorefineries: traditional, recent, and forthcoming approaches to convert raw lignocellulose into valuable materials and chemicals. *RSC Sustain.* 2 (1), 37–90. doi:10.1039/D3SU00140G

Chu, Q., Tong, W., Chen, J., Wu, S., Jin, Y., Hu, J., et al. (2021). Organosolv pretreatment assisted by carbocation scavenger to mitigate surface barrier effect of lignin for improving biomass saccharification and utilization. *Biotechnol. Biofuels* 14 (1), 136. doi:10.1186/s13068-021-01988-w

da Costa, R. M. F., Pattathil, S., Avci, U., Lee, S. J., Hazen, S. P., Winters, A., et al. (2017). A cell wall reference profile for Miscanthus bioenergy crops highlights compositional and structural variations associated with development and organ origin. *New Phytol.* 213 (4), 1710–1725. doi:10.1111/nph.14306

Damm, T., Pattathil, S., Günl, M., Jablonowski, N. D., O'Neill, M., Grün, K. S., et al. (2017). Insights into cell wall structure of Sida hermaphrodita and its influence on recalcitrance. *Carbohydr. Polym.* 168, 94–102. doi:10.1016/j.carbpol.2017.03.062

Eickenscheidt, T., Bockermann, C., Bodenmüller, D., Großkinsky, T., Gutermuth, S., Hafner, M., et al. (2023). *MOORuse - Paludikulturen für Niedermoorböden in Bayern - Etablierung, Klimarelevanz and Umwelteffekte, Verwertungsmöglichkeiten und Wirtschaftlichkeit, Abschlussbericht*, 254. doi:10.5281/zenodo.10778063.2

Fincher, G. B. (2009). Revolutionary times in our understanding of cell wall biosynthesis and remodeling in the grasses. *Plant Physiol.* 149 (1), 27–37. doi:10.1104/pp.108.130096

Foster, C. E., Martin, T. M., and Pauly, M. (2010a). Comprehensive compositional analysis of plant cell walls (Lignocellulosic biomass) part I: lignin. *J. Vis. Exp.* (37), 1745. doi:10.3791/1745

Foster, C. E., Martin, T. M., and Pauly, M. (2010b). Comprehensive compositional analysis of plant cell walls (Lignocellulosic biomass) part II: carbohydrates. *J. Vis. Exp.* (37), 1837. doi:10.3791/1837

Fry, S. C., Nesselrode, B. H. W. A., Miller, J. G., and Mewburn, B. R. (2008). Mixed-linkage (1→3,1→4)-β-D-glucan is a major hemicellulose of Equisetum (horsetail) cell walls. *New Phytol.* 179 (1), 104–115. doi:10.1111/j.1469-8137.2008.02435.x

Gismatulina, Y. A., Budaeva, V. V., Kortusov, A. N., Kashcheyeva, E. I., Gladysheva, E. K., Mironova, G. F., et al. (2022). Evaluation of chemical composition of miscanthus × giganteus raised in different climate regions in Russia. *Plants* 11 (20), 2791. doi:10.3390/plants11202791

Giummarella, N., Zhang, L., Henriksson, G., and Lawoko, M. (2016). Structural features of mildly fractionated lignin carbohydrate complexes (LCC) from spruce. *RSC Adv.* 6 (48), 42120–42131. doi:10.1039/c6ra02399a

Giummarella, N., Pu, Y., Ragauskas, A. J., and Lawoko, M. (2019). A critical review on the analysis of lignin carbohydrate bonds. *Green Chem.* 21 (7), 1573–1595. doi:10.1039/C8GC03606C

Grande, P. M., Viell, J., Theyssen, N., Marquardt, W., Domínguez de María, P., and Leitner, W. (2015). Fractionation of lignocellulosic biomass using the OrganoCat process. *Green Chem.* 17 (6), 3533–3539. doi:10.1039/c4gc02534b

Grande, P. M., Weidener, D., Dietrich, S., Dama, M., Bellof, M., Maas, R., et al. (2019). OrganoCat fractionation of empty fruit bunches from palm trees into lignin, sugars, and cellulose-enriched pulp. *ACS Omega* 4 (11), 14451–14457. doi:10.1021/acsomega.9b01371

Hatfield, R. D., Rancour, D. M., and Marita, J. M. (2017). Grass cell walls: a story of cross-linking. *Front. Plant Sci.* 7, 2056. doi:10.3389/fpls.2016.02056

Himmel, M. E., Ding, S. Y., Johnson, D. K., Adney, W. S., Nimlos, M. R., Brady, J. W., et al. (2007). Biomass recalcitrance: engineering plants and enzymes for biofuels production. *Science* 315 (5813), 804–807. doi:10.1126/science.1137016

Janyszek-Sołtysiak, M., Grzelak, M., Gajewski, P., Jagodziński, A. M., Gaweł, E., and Wrońska-Pilarek, D. (2021). Mineral contents in aboveground biomass of sedges (Carex L., Cyperaceae). *Energies* 14 (23), 8007. doi:10.3390/en14238007

Klose, H., and Paës, G. (2023). Editorial: understanding plant cell wall recalcitrance for efficient lignocellulose processing. *Front. Plant Sci.* 14 (October), 1–3. doi:10.3389/fpls.2023.1284658

Lawoko, M., Henriksson, G., and Gellerstedt, G. (2005). Structural differences between the lignin–carbohydrate complexes present in wood and in chemical pulps. *Biomacromolecules* 6 (6), 3467–3473. doi:10.1021/bm058014q

Leifeld, J., and Menichetti, L. (2018). The underappreciated potential of peatlands in global climate change mitigation strategies. *Nat. Commun.* 9 (1), 1071. doi:10.1038/s41467-018-03406-6

Lever, M. (1972). A new reaction for colorimetric determination of carbohydrates. *Anal. Biochem.* 47 (1), 273–279. doi:10.1016/0003-2697(72)90301-6

Lewandowski, I., Clifton-Brown, J., Trindade, L. M., van der Linden, G. C., Schwarz, K. U., Müller-Sämann, K., et al. (2016). Progress on optimizing miscanthus biomass production for the European bioeconomy: results of the EU FP7 project OPTIMISC. *Front. Plant Sci.* 7, 1620. doi:10.3389/fpls.2016.01620

Li, Y., Tao, L., Nagle, N., Tucker, M., Chen, X., and Kuhn, E. M. (2022). Effect of feedstock variability, feedstock blends, and pretreatment conditions on sugar yield and production costs. *Front. Energy Res.* 9 (January), 1–12. doi:10.3389/fenrg.2021.792216

Liu, Y., Deak, N., Wang, Z., Yu, H., Hameleers, L., Jurak, E., et al. (2020). Tunable and functional deep eutectic solvents for lignocellulose valorization. *Nat. Commun.* 12, 5424 doi:10.1038/s41467-021-25117-1

Martinez Diaz, J., Grande, P. M., and Klose, H. (2023). Small-scale OrganoCat processing to screen rapeseed straw for efficient lignocellulose fractionation. *Front. Chem. Eng.* 5, 1098411. doi:10.3389/fceng.2023.1098411

Parish, F., Sirin, A., Charman, D., Joosten, H., Minayeva, T., and Silvius, M., , et al. (2008). *Assessment on Peatlands, Biodiversity and Climate Change: Main Report* (Kuala Lumpur: Wageningen: Global Environment Centre, Kuala Lumpur and Wetlands International, Wageningen).

Ragauskas, A. J., Beckham, G. T., Biddy, M. J., Chandra, R., Chen, F., Davis, M. F., et al. (2014). Lignin valorization: improving lignin processing in the biorefinery. *Science* 344 (6185), 1246843. doi:10.1126/science.1246843

Ralph, J., Lundquist, K., Brunow, G., Lu, F., Kim, H., Schatz, P. F., et al. (2004). Lignins: natural polymers from oxidative coupling of 4-hydroxyphenyl-propanoids. *Phytochem. Rev.* 3, 29–60. doi:10.1023/B:PHYT.0000047809.65444.a4

Rodriguez-Dominguez, M. A., Bonefeld, B. E., Ambye-Jensen, M., Brix, H., and Arias, C. A. (2022). The use of treatment wetlands plants for protein and cellulose valorization in biorefinery platform. *Sci. Total Environ.* 810, 152376. doi:10.1016/j.scitotenv.2021.152376

Schäfer, J., Sattler, M., Iqbal, Y., Lewandowski, I., and Bunzel, M. (2019). Characterization of miscanthus cell wall polymers. *GCB Bioenergy* 11 (1), 191–205. doi:10.1111/gcbb.12538

Schellekens, J., Buurman, P., and Kuyper, T. W. (2012). Source and transformations of lignin in Carex-dominated peat. *Soil Biol. Biochem.* 53, 32–42. doi:10.1016/j.soilbio.2012.04.030

Schoofs, L., Weidener, D., Schurr, U., Klose, H., and Grande, P. M. (2021). Fractionation of lignocellulosic biomass using the organocat process. *J. Vis. Exp.* 2021 (172), 1–12. doi:10.3791/61933

Schoofs, L., Thiele, B., Tonn, J., Langletz, T., Herres-Pawlis, S., Jupke, A., et al. (2024). Structural changes of lignin during OrganoCat processing. *Energy Fuels* 38 (5), 4192–4202. doi:10.1021/acs.energyfuels.3c03673

Scott, T. A., and Melvin, E. H. (1953). Determination of dextran with anthrone. *Anal. Chem.* 25 (11), 1656–1661. doi:10.1021/ac60083a023

Strašil, Z., Váňa, V., and Káš, M. (2005). The reed canary grass (Phalaris arundinacea L.) cultivated for energy utilization. *Res. Agric. Eng.* 51 (1), 7–12. doi:10.17221/4895-RAE

Suzuki, K., Kitamura, S., Kato, Y., and Itoh, T. (2000). Highly substituted glucuronoarabinoxylans (hsGAXs) and low-branched xylans show a distinct localization pattern in the tissues of Zea mays L. *Plant Cell Physiology* 41 (8), 948–959. doi:10.1093/pcp/pcd019

Tarasov, D., Leitch, M., and Fatehi, P. (2018). Lignin–carbohydrate complexes: properties, applications, analyses, and methods of extraction: a review. *Biotechnol. Biofuels* 11 (1), 269. doi:10.1186/s13068-018-1262-1

Terrett, O. M., and Dupree, P. (2019). Covalent interactions between lignin and hemicelluloses in plant secondary cell walls. *Curr. Opin. Biotechnol.* 56, 97–104. doi:10.1016/j.copbio.2018.10.010

Uellendahl, K., Hirschelmann, S., and Abel, S. (2023). *Treibhausgas-Emissionen der Moorreichen Bundesländer Und Die Rolle Der Organischen Böden*. Greifswald. Available online at: https://www.greifswaldmoor.de/files/dokumente/Infopapiere_Briefings/202305_FaktenpapierEmissionenBundesländer_final_korr.pdf (Accessed December 12, 2025).

UNEP (2022). Global peatlands assessment: the state of the world's peatlands - evidence for action toward the conservation, restoration, and sustainable management of peatlands. *U. N. Environ. Programme*, 1–418. doi:10.59117/20.500.11822/41222

Updegraff, D. M. (1969). Semimicro determination of cellulose inbiological materials. *Anal. Biochem.* 32 (3), 420–424. doi:10.1016/S0003-2697(69)80009-6

Vanholme, R., Demedts, B., Morreel, K., Ralph, J., and Boerjan, W. (2010). Lignin biosynthesis and structure. *Plant Physiol.* 153 (3), 895–905. doi:10.1104/pp.110.155119

Vogel, J. (2008). Unique aspects of the grass cell wall. *Curr. Opin. Plant Biol.* 11 (3), 301–307. doi:10.1016/j.pbi.2008.03.002

Waliszewska, B., Janyszek, M., Grzelak, M., Gaweł, E., et al. (2013). Characteristic of thermochemical parameters of aboveground parts of selected sedges. *Carex L . Cyperaceae* 5 (4), 1–6.

Weidener, D., Dama, M., Dietrich, S. K., Ohrem, B., Pauly, M., Leitner, W., et al. (2020). Multiscale analysis of lignocellulose recalcitrance towards OrganoCat pretreatment and fractionation. *Biotechnol. Biofuels* 13 (1), 155. doi:10.1186/s13068-020-01796-8

Weidener, D., Leitner, W., Domínguez de María, P., Klose, H., and Grande, P. M. (2021). Lignocellulose fractionation using recyclable phosphoric acid: lignin, cellulose, and furfural production. *ChemSusChem* 14 (3), 909–916. doi:10.1002/cssc.202002383

Wichmann, S., and Nordt, A. (2024). Unlocking the potential of peatlands and paludiculture to achieve Germany's climate targets: obstacles and major fields of action. *Front. Clim.* 6 (1380625), 1380625. doi:10.3389/fclim.2024.1380625

Wichtmann, W., and Joosten, H. (2007). Paludiculture: peat formation and renewable resources from rewetted peatlands. *IMCG Newsl.*, 24–28.

Wilson, D., Blain, D., Couwenberg, J., Evans, C., Murdiyarso, D., Page, S., et al. (2016). Greenhouse gas emission factors associated with rewetting of organic soils. *Mires Peat* 17 (4), 04. doi:10.19189/MAP.2016.OMB.222

Woiciechowski, A., Dalmas Neto, C. J., Porto de Souza Vandenberghe, L., de Carvalho Neto, D. P., Novak Sydney, A. C., Letti, L. A. J., et al. (2020). Lignocellulosic biomass: acid and alkaline pretreatments and their effects on biomass recalcitrance – conventional processing and recent advances. *Bioresour. Technol.* 304 (January), 122848. doi:10.1016/j.biortech.2020.122848

Yu, Z. C. (2012). Northern peatland carbon stocks and dynamics: a review. *Biogeosciences* 9 (10), 4071–4085. doi:10.5194/bg-9-4071-2012

Zeng, Y., Zhao, S., Yang, S., and Ding, S. Y. (2014). Lignin plays a negative role in the biochemical process for producing lignocellulosic biofuels. *Curr. Opin. Biotechnol.* 27, 38–45. doi:10.1016/j.copbio.2013.09.008

Zhang, Y., Li, M., Nie, T., and Ni, Z. (2018). A process study of lactic acid production from phragmites australis straw by a thermophilic bacillus coagulans strain under non-sterilized conditions. *Processes* 6 (10), 11–13. doi:10.3390/pr6100175

Zhao, X., Zhang, L., and Liu, D. (2012). in *Biomass Recalcitrance. Part I: The Chemical Compositions and Physical Structures Affecting the Enzymatic Hydrolysis of Lignocellulose*, 465–482. doi:10.1002/bbb.1331

Ziegler, R., Wichtmann, W., Abel, S., Kemp, R., Simard, M., and Joosten, H. (2021). Wet peatland utilisation for climate protection – an international survey of paludiculture innovation. *Clean. Eng. Technol.* 5, 100305. doi:10.1016/j.clet.2021.100305

10.3389/fceng.2026.1799905

Appendix

TABLE A1 Yields of alcohol-soluble components and starch (% of dried plant material) during the pretreatment (dAIR-process) of the biomass prior to analyses.

	Miscanthus	*Phragmites*	*Carex*	*Phalaris*
Alcohol-soluble components	8.5	10.1	21.1	22.8
Starch	6.8	6.8	10.5	10.5